Force sensing and transmission in human induced pluripotent stem-cell-derived pericytes

Iendaltseva, O.

Chapter 5

Pericyte force generation in *in vitro* Hypoxia and Ischemia conditions [1]

abstract

Pericytes (PCs) are contractile cells that align blood microvessels. Their contractility plays an important role in physiology and pathology. For example in Ischemia, PCs have been shown to die shortly after they constrict capillaries in response to compromised oxygen and glucose supply. Consequently, capillaries are blocked by dead, constricted PCs further reinforcing the diseased condition leading to large-area brain damage after a stroke.

The essential cells involved in Ischemia are mid-capillary PCs that are difficult to study specifically as of the absence of unique markers, hence studies are limited to *in vivo*, post-event investigations. In particular the constriction model is difficult to asses since it is not possible to measure directly the forces PCs apply at a high level of control over the experimental conditions *in vivo*.

Here we developed and described a novel approach that allows to accurately monitor cellular forces and morphology, while rapidly changing microenvironmental conditions. By integrating PDMS micropillar arrays inside of fluid-flow channels and using human induced pluripotent stem cell (hiPSC)-derived PCs, we brought *in vitro* experiments closer

1. This chapter is based on: O. Iendaltseva, V.V. Orlova, C.L. Mummery, E. H. J. Danen and T. Schmidt, Pericyte Force Generation in *In Vitro* Hypoxia and Ischemia Conditions, *In preparation*

to *in vivo* studies on Ischemia. The developed methodology does create an opportunity to track PC mechanoresponse to changes in oxygen and glucose supply in a real-time setting for future applications.

5.1 Introduction

Pericytes (PC) are mural cells of blood microvessels. They are isolated contractile cells involved in regulation of vascular morphogenesis and function in health and disease [1]. Among others, PCs are involved in Hypoxia induced angiogenesis in physiology (e.g. embryo development), and in pathology (e.g. tumour or tissue injury) [2]. Additionally, despite some contradictory results, they have been reported to participate in regulation of cerebral blood flow and promote brain damage in Ischemia in mice *in vivo* [3–5]. PCs have been shown to die shortly after they constrict capillaries in response to Ischemia, thus preventing renewal of the blood flow through capillary bed and damage of the neurons after stroke. Nevertheless, there is no direct evidence in terms of direct mechanical measurements of whether PCs are able to block capillary blood flow in Ischemia or not.

Therefore we first assessed the contractility of PCs in *in vitro* Hypoxia and Ischemia conditions, and compared those to the normal conditions.

Metazoan organisms use oxygen (O_2) for adenosine triphosphate (ATP) production. It is necessary to maintain O_2 homeostasis for proper organism development, physiology and function. A decrease in O_2 supply results in a condition called Hypoxia [6]. A subsequent response to Hypoxia in cells and tissues is regulated by the family of Hypoxia-inducible factor (HIF) transcription factors. HIFs are heterodimeric proteins composed of two subunits: one α (HIF-1α, HIF-2α, HIF-3α) and one β (HIF-β/ARNT). HIF-1α and HIF-2α play a central role in cellular response to Hypoxia [7]. O_2 deprivation stabilizes transcription factor HIF-1α and HIF-2α, which in turn regulate the expression of hundreds of genes to maintain O_2 homeostasis. This includes: glucose metabolism, cell proliferation, migration, cytoskeletal structure, metastasis, apoptosis, angiogenesis, extracellular matrix formation and remodeling, etc. Under normoxia conditions HIF-α is continuously produced and degraded by binding of the von Hippel-Lindau tumor suppressor protein (VHL) that interacts with the protein Elongin C, recruiting an E3 ubiquitin-protein ligase complex leading to HIF-α ubiquitination and degradation by the 26S proteasome. While in Hypoxia conditions, HIF-α degradation is inhibited due to the lack of oxygen. The protein accumulates, binds to HIF-β, translocates to the nucleus and activates Hypoxia-response gene transcription [2, 8].

Compromised blood supply in tissue leads to a decreased oxygen

and nutrients delivery, and results in a condition called Ischemia. In Ischemia, cells switch from aerobic to anaerobic metabolism that leads to a reduction of cell pH, high inflow of sodium ions into cells, depletion of cellular ATP and inactivation of ATPases, inhibition of Ca^{2+} outflow and intracellular calcium overload, opening of the mitochondrial permeability transition (MPT) pore and further impairment of ATP production. The degree of tissue injury depends on the organ, the level and duration of blood supply reduction [9].

To avoid heterogenity in PC cell culture, present in *in vivo* studies, we used human induced pluripotent stem cell (hiPSC)-derived PCs, that have been previously described and characterized in detail [10, 11]. The cells lack α-SMA expression and resemble "true" PCs, which have been found on mid-capillaries.

For simulation of Hypoxia and Ischemia conditions we used a chemical mimetic. Cells were treated with an indirect HIF-inhibitor DMOG that switches cells into a Hypoxia state, and we used glucose deprivation to switch cells to their starvation and Ischemia state. Indeed we were able to define a mechanical response that was specific to the different treatments.

However, our results showed that this static approach does not allow to accurately measure the fast response of PCs that occurs during the acute medical condition. To better simulate rapid changes in oxygen and glucose levels during Hypoxia and Ischemia, and to get our experiments closer to the aforementioned *in vivo* studies, we further developed and characterized a new experimental design. In this new design PDMS micropillar arrays are mounted inside commercially available fluid-flow channels. Cells are seeded on top of the micropillar arrays. Our novel approach allows to constantly track cellular forces and morphology while dynamically changing the environmental conditions such as: the temperature, the composition of the cell culture medium, and the oxygen concentration.

The novel approach presented in this chapter, is a ubiquitous design that permits the study of PCs behaviour during hypoxia and ischemia. It also can be applied to any other cells for which the environmental conditions needs to be changed, and where response in cell force application and morphology are questioned.

5.2 Methods

5.2.1 Cell culture

hiPSC line LUMC06iCTRL-derived CD31– (dif31), cell line was cultured in Dulbecco's Modified Eagle's Medium (DMEM, Gibco|Thermo Fisher Scientific, USA) supplemented with 10% fetal bovine serum (HyClone, Etten-Leur, The Netherlands), 25 U/ml penicillin and 25 µg/ml streptomycin (Invitrogen/Fisher Scientific). CD31– cell line was used on the passage 7 or 8 and was kept in culture for 3 to 4 days before the experiment to avoid changes in the cell morphology. Cells were seeded at 20 000 cells per dish. Cells were injected directly on top of the PDMS microropillar area of interest to ensure persistent cell density across experiments. After incubation they were fixed for 10' in 4% paraformaldehyde in PBS for further immunostaining.

Simulated Hypoxia

Hypoxia was simulated by chemical stabilization of HIF-α. CD31– cells were, first, incubated for 40 hours with dimethyloxalylglycine (DMOG, Sigma-Aldrich, d3695) added to the full culture media at 1 mM concentration. Then, they were detached from the culture dish using PBS and Trypsin with 1 mM DMOG. Finally, CD31– cells were seeded on top of the PDMS micropillar arrays in culture media containing 1 mM DMOG and 4.5 g/l D-glucose concentrations and fixed after 8.5 hours of spreading.

Simulated Ischemia

Ischemia was simulated by simultaneous chemical stabilization of HIF-α together with glucose deprivation from the culture media. CD31– cells were, first, incubated for 40 hours with dimethyloxalylglycine (DMOG, Sigma-Aldrich, d3695) added to the full culture media (DMEM, Gibco| Thermo Fisher Scientific, USA) at 1 mM concentration. Then, they were detached from the culture dish using PBS and Trypsin with 1 mM DMOG. Finally, CD31– cells were seeded on top of the PDMS micropillar arrays in the full cell culture media containing 1 mM DMOG for 7 hours. After 7 hours the media was exchanged with a low 1 g/l D-glucose cell culture medium (DMEM, Gibco | Thermo Fisher Scientific,

USA) containing 1 mM DMOG concentration and fixed after 1.5 hours of spreading in Ischemia conditions.

Starvation

Cell starvation was simulated by using low glucose culture media. CD31– cells were, first, incubated for 40 hours in full high glucose (4,5 g/l) media. Then, they were detached from the culture dish and placed on top of the PDMS micropillars arrays in a culture media containing low 1 g/l D-glucose. After 8.5 hours of incubation cells were fixed.

5.2.2 PDMS micropillar array preparation

PDMS micropillar arrays were prepared as was described before [12, 13]. Briefly, SI mold was made by two-step Deep Reactive Ion Etching (DRIE) process. This yielded a 10×10 mm hexagonal array of 2 μm diameter holes with 2 μm spacing and varying depth, flanked by two 50 μm deep 10×2 mm tranches. After mold passivation with trichloro silane (Sigma), PDMS 1:10 was poured over it and cured for 20 hours at 110°C. The peeled off PDMS had a negative of the mold shape with micropillar array and 50 μm high spacers on the sides of it. This array was functionalized with the help of PDMS 1:30 stamp and dried protein of interest on top of it. A 40 μl drop of FN or LM-111 mixture in water was incubated for 60' on the PDMS 1:30 stamp, then washed and dried under laminar flow. This stamp was then genly loaded onto UV-ozone activated PDMS micropillar array for 10'. Finally, stamped array was blocked with 0.2% Pluronic (F-127, Sigma) in PBS for 60' at room temperature and washed with PBS.

5.2.3 Immunostaining

Fixed cells were permeabilized for 10' with 0.1% Triton-X in PBS and blocked for 60' with 1% bovine serum albumin (BSA) (Sigma, a2153) in PBS. F-actin cytoskeleton of cells was stained for 1 hour with Alexa 532 phalloidin (Thermo Fisher Scientific, a22282) of a 1:1000 concentration in PBS. Cell nuclei were stained for 1 hour using 300 nM solution of 4',6-diamidino-2-phenylindole (DAPI, Sigma-Aldrich, d8417) in PBS. Each immunostaining step was followed by 3 washing steps in PBS 10' each under a gentle rocking.

5.2.4 Microscopy

Confocal imaging was performed on a home-built setup based on an Axiovert200 microscope body (Zeiss), spinning disk unit (CSU-X1, Yokogawa) and an emCCD camera (iXon 897, Andor). IQ-software enabled setup-control and data acquisition. Lasers of 405 nm (CrystaLaser), 488 nm (Coherent), 514 nm, 561 nm (Cobolt) and 642 nm (Spectra Physics) wavelength were coupled into the CSU via polarization maintaining single-mode fiber. Spacers on the sides of micropillar arrays allowed placing them upside down onto #0 coverslips (Menzel Glaser) with adhered cells facing down. This approach ensured reproducible cell observation within the limited working distance of a high-NA objective on an inverted microscope. For PDMS or glass 2D assays parafilm spacers were made directly on top of the glass coverslips.

5.2.5 Image analysis

Cell spreading area and nucleus size were quantified by using FIJI software. First the background was subtracted by adjusting the threshold level, followed by the cell/nucleus edge selection with a tracing tool. Finally mean values for at least 30 cells per condition were calculated.

Cell traction forces were measured by using micropillar array technology [13–15] and quantified as previously described [12]. Micropillar tops were functionalized with fluorescently labeled FN or with LM that was labeled subsequently bu immunostaining. This allowed us to detect deflections with ∼30 nm accuracy corresponding to 500 pN for soft and 2 nN for stiff pillars force precision by using a specifically designed Matlab script.

5.2.6 Preparation of flow channels with encapsulated PDMS micropillar arrays

First, the Si mold with one 10 × 10 mm hexagonal array of 2 µm diameter holes with 2 µm spacing and varying depth, flanked by two 50 µm deep 10×2 mm tranches was passivated with trichloro silane (Sigma). Then a titanium mold with ∼350 µm deep 20 × 20 mm square recess was also passivated with trichloro silane (Sigma). The two molds were brought into contact and fixed against each other (Fig. 5.4a). PDMS 1:10 was poured over SI mold via the one of the two holes in the titanium mold with the help of a pipette (Fig. 5.4b), degassed for 1 hour and

cured for 20 hours at 110°C (Fig. 5.4c). After curing the titanium mold was gently removed (Fig. 5.4d) and PDMS was peeled off the SI mold (Fig. 5.4e). All excess of PDMS was cut off to leave only a 10×10 micropillar array and 50 μm high spacers (Fig. 5.4f). Further, the PDMS micropillar array was divided into two halves along the long side (Fig. 5.4g). From each half of the micropillar array a middle third of spaces was deleted to make sure fluid can pass through (Fig. 5.4h, i). To make sure no flow was present on the side of the PDMS micropillar arrays a small amount of PDMS 1:30 was spread with the help of a pipette inside fluid flow channels of the Ibidi slide (Ibidi, 80608) (Fig. 5.5a). The so prepared micropillar arrays were immediately placed inside the channels and cured for 30' at 60°C (Fig. 5.5b). The two halves of a micropillar array were further functionalized with the help of PDMS 1:30 stamps and FN on top of them. A 40 μl drop of FN mixture in water was incubated for 60' on PDMS 1:30 stamps, then washed and dried in a laminar flow (Fig. 5.5c). The stamps were then gently loaded onto UV-ozone activated PDMS micropillar array halves for 10' (Fig. 5.5d-e). Finally, the flow channels were closed with the help of a #0 coverslip applied to the sticky bottom of the Ibidi slide (Fig. 5.5g). The stamped arrays were subsequently blocked with 0.2% Pluronic (F-127, Sigma) in PBS for 60' at room temperature and washed with PBS.

5.2.7 Seeding cells on top of PDMS micropillar arrays inside flow channels

Before seeding hiPSC line LUMC06iCTRL-derived CD31– (dif31) cells, a Ibidi slide with PDMS micropillar arrays inside was washed with PBS (Fig. 5.6a). Then, Dulbecco's Modified Eagle's Medium (DMEM, Gibco|Thermo Fisher Scientific, USA) supplemented with 10% fetal bovine serum (HyClone, Etten-Leur, The Netherlands), 25 U/ml penicillin and 25 μg/ml streptomycin (Invitrogen/Fisher Scientific) containing 20 000 CD31– cells per sample was injected into each flow channel with the help of a pipette (Fig. 5.6b). Channels were finally closed with a lid provided together with the Ibidi slide (Fig. 5.6c). The slide was further controlled under the microscope for homogeneous cell distribution inside each flow channel, flipped over for the coverslip to face upwards and placed in an incubator for 1 hour for cells to adhere to PDMS micropillars (Fig. 5.6d). After cell attachment the slide was imaged in the INUBGE2E-ZILCS (TokiaHit, Japan) that allows to change CO_2 level

(Fig. 5.6e).

5.3 Results

5.3.1 Pericyte force generation and spreading in starvation, Hypoxia and Ischemia conditions

First we assessed PC force generation and spreading in static, chemically simulated Hypoxia, starvation and Ischemia conditions. Starvation was simulated by incubating PCs in a cell culture media containing low 1 g/l D-glucose. Hypoxia was simulated by treating PCs with 1 mM dimethyloxalylglycine (DMOG), which inhibits prolyl hydroxylases (PHDs) and stabilises HIF-1. Ischemia was simulated by combing DMOG treatment with incubation in a low glucose media.

To investigate an effect of the cell culture media with a low glucose concentration on PC force application we run a starvation experiment. First, PCs were seeded on top of the 47.2 kPa stiff PDMS micropillar arrays and allowed to attach and spread for 7 hours in a full media. Then, cell culture media was replaced with a low glucose media. After 1.5 hours in a low glucose media PCs were fixed and stained for F-actin.

For the simulation of Hypoxia, we first identified the DMOG concentrations that were not cytotoxic for PCs. We evaluated PCs viability for DMOG concentrations of 0.125, 0.5, 1.0, 1.5, 2.0, and 3.0 mM. Our results showed that DMOG concentrations above 1 mM were cytotoxic for PCs. For our further experiments we chose DMOG concentration of 1 mM. Our viability results corroborate findings of earlier studies [16–18].

PCs were incubated for 40 hours in a cell culture medium with 1 mM DMOG to stabilize HIF-1. Then, PCs were detached from the culture dish using PBS and trypsin with 1 mM DMOG concentration to make sure HIF-1 accumulation in the nucleus is not disturbed. Finally, PCs were seeded on top of the 47.2 kPa stiff PDMS micropillar arrays in a cell culture media containing 1 mM DMOG and incubated for 8.5 hours before fixation. After fixation, PCs were immunostained for F-actin.

To test PCs force response in Ischemia conditions PCs were prepared in a similar way as for Hypoxia experiment. They were treated, first, with 1 mM DMOG for 40 hours. Then, seeded on top of the 47.2 kPa stiff PDMS micropillar arrays using PBS and Trypsin with 1 mM DMOG concentration. After 7 hours of incubation in a full cell culture media

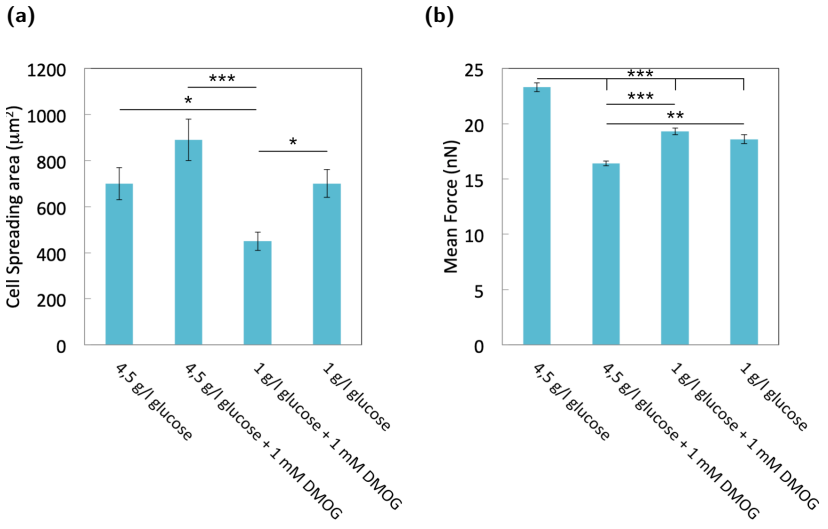

Figure 5.1: Average cell spreading area and force application of PCs. (a) – Average cell spreading area of PCs in normoxia (4.5 g/l glucose), Hypoxia (4.5 g/l glucose + 1 mM DMOG), Ischemia (1 g/l glucose + 1 mM DMOG) and starvation (1 g/l glucose) conditions. (b) – Average fore application of PCs in normoxia, Hypoxia, Ischemia and starvation (1 g/l glucose) conditions. Results are derived from three experiments performed in two replicates. NS, $P>0.05$; *$P<0.05$; **$P<0.005$; ***$P<0.0005$ according to T-test.

containing 1 mM DMOG PC were placed in Ischemia conditions by changing cell culture media to a low 1 g/l D-glucose media containing 1 mM DMOG. Finally, PCs were fixed after 1.5 hours in Ischemia conditions and stained for F-actin.

For control samples PCs were incubated on top of the 47.2 kPa stiff PDMS micropillar arrays in a full cell culture media for 8.5 hours, then fixed and immunostained for F-actin cytoskeleton.

Our results showed an about 20% larger cell spreading area, and an about 30% lower force application of PCs placed in simulated Hypoxia conditions (4.5 g/l glucose + 1 mM DMOG) as compared to the control sample (4.5 g/l glucose) (Fig. 5.1a, 5.1b). After 1.5 hours in Ischemia conditions (1 g/l glucose + 1 mM DMOG) PCs showed the lowest spreading area compared to control, Hypoxia and starvation (1 g/l glucose) samples (Fig. 5.1a). Force application of PCs in Ischemia conditions rapidly increased by $\sim$ 15% compared to PCs in Hypoxia (Fig. 5.1b. Many dead cells were found after 1.5 hours in Ischemia conditions.

In starvation cell spreading area of PCs was comparable to the control sample (Fig. 5.1a), while force application slightly decreased (Fig. 5.1b).

As can be seen from our data, the behavior of PCs changes rapidly (within 1.5 hours) when cells are placed in Ischemia conditions. Unfortunately, Ischemia can't be simulated as an immediate event using the described chemical inhibition method that requires a long pre-treatment with DMOG. Thus, for short-term experiments, that reflects the situation in medical condition, we needeeded to develop another approach that would allow us to constantly monitor the cellular forces, while cells are challenged by deprivation of oxygen and glucose.

5.3.2 Micropillar array technology does not allow fast liquid exchange in the area with cells

The PDMS micropillar array technology developed by us, which permits to study cellular mechanotransduction on a high-resolution microscope, required that micropillar arrays to be flipped upside down to face the objective of a microscope. In this way a precise measurement of cellular forces is achieved [12]. Here we tested whether it was feasible to rapidly change cell culture media located in the 50 μm space between the micropillar arrays and the coverslip in a rapid and reliable manner.

We first analyzed whether the liquid on top of the micropillar arrays could be homogenized by diffusion. Given the size of the arrays, $A = (10 \times 10)mm^2$, and given a typical diffusion constant of $D = 100\ \mu m^2/s$ for a small molecule like a fluorescence dye, it will take, $t = A/(4D) \approx 70\ h$. Hence, a fast medium exchange cannot rely on diffusion.

This prediction was corroborated in experiments. A micropillar array was flipped and fixed against a coverslip of the commercially available dish with a glass bottom. The dish was filled with a PBS solution containing a fluorophore. Under constant monitoring, the PBS solution was replaced with a new – fluorophore-free PBS. The sample was then monitored for a change in the fluorophore signal between pillars and the coverslip. We found that days were required for the new PBS solution to diffuse under the array. This was due to the tiny opening $< 50\ \mu m$ between the micropillars and the coverslip provided by spacers flanking the array and the absence of any fluid flow. Interchange of liquid is solely driven by diffusion.

Thus, it is not possible to rapidly exchange cell culture media surrounding PCs on micropillars and constantly monitor cellular forces in a

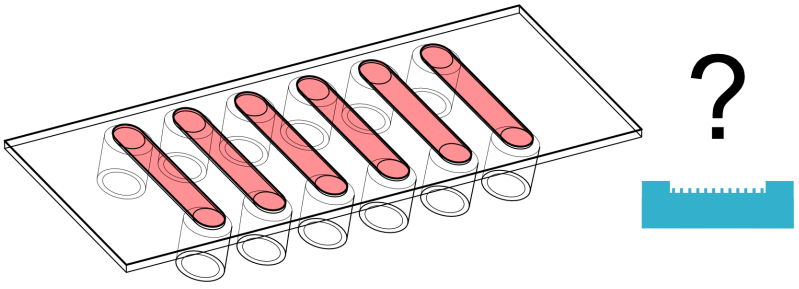

Figure 5.2: Combining micropillar array technology with fluid flow channels would allow to monitor cellular forces and morphology under dynamically changing conditions.

given setup in the envisioned timescale of several minutes. In particular such approach does not fit the requirements of Hypoxia and Ischemia experiments and a new method needed to be developed to permit fast exchange of the cell culture media between micropillars and the coverslip.

5.3.3 Design of a microfluidic channel to track cellular response in rapidly changing conditions

Commercially available slides with fluid flow channels allow cell monitoring under changing conditions, but not cell force measurements. Combining micropillar array technology with fluid flow channels would allow to monitor cellular forces and morphology and simultaneously change cell culture media content. Additionally, micropillar arrays of different stiffness could be used for such experiments (Fig. 5.2). Here we combined two technologies to get a tool that can be used to track fast response of PCs to ischemia conditions *in vitro*.

Requirements

We started by defining requirements for the new design. It had to resemble benefits and functionalities of both techniques. The requirements identified were: (i) the micropillar arrays had to be fitted in a given fluid flow channel, (ii) the design had to allow the fluid to flow in between pillars and a coverslip only, as to make sure that media is effectively replaced in the volume around cells, (iii) the distance from the coverslip

to the pillars had to stay $\sim 50\ \mu m$ to allow high-resolution force measurements, (iv) the fluid flow channel had to allow using #0 coverslips to facilitate imaging with high numerical aperture (NA) objectives.

Design decisions

We chose to use commercially available slides with six fluid flow channels 0.4 mm deep, 17 mm long and 3.8 mm wide, and a self-adhesive side to mount own coverslips. Due to an open design these slides allowed us to put pillars inside and close channels with #0 coverslips to satisfy requirements (i) and (iv).

We decided to cut micropillar arrays in half along the long edge to fill in two channels at a time and keep 50 μm spacers to provide a fixed distance between a coverslip and pillars. This decision was taken to satisfy requirement (iii).

To have a fluid flow between pillars and a coverslip we chose to make an $\sim 1.7\ mm$ opening in the spacers on both sides of a micropillar array. To satisfy requirement (ii) we decided to create an additional mold to prepare micropillar arrays of a fixed thickness corresponding the depth of the prefabricated channels – 0.4 mm.

A schematic drawing of a final design is given in figure 5.3.

5.3.4 Channel preparation

The mold

First, we started to prepare a mold to produce micropillar arrays of a fixed thickness to fit inside fluid flow channels. A new mold had to be applied on top of a silicon wafer containing $10 \times 10\ mm$ hexagonal array of 2 μm diameter holes with 2 μm spacing and varying depth, flanked by two 50 μm deep $10 \times 2\ mm$ tranches – a negative of a PDMS micropillar array. Taking into account the 0.4 mm deep fluid flow channels and the 50 μm high micropillar array spacers the new mold needed to have a 0.35 mm deep recess such that arrays may fit in the channel (Fig. 5.4a). Additionally, the mold had to contain openings to insert PDMS after fixing the mold and a silicon wafer against each other (Fig. 5.4b).

We tested a number of different designs and materials for the mold (Fig. 5.11). Finally, we produced a mold made of a titanium. Titanium is resistant to chloride ions and other chemicals used during PDMS micropillar array production. A square $40 \times 40\ mm$ mold was produced

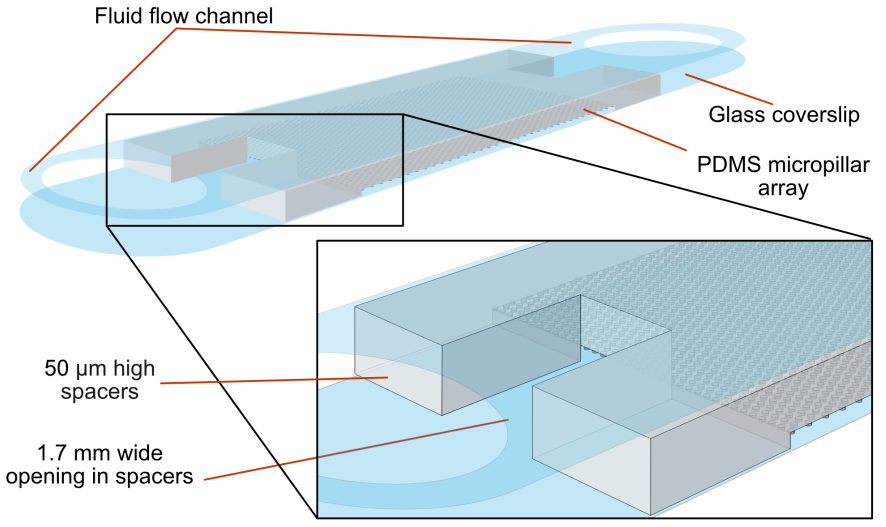

Figure 5.3: A schematic representation of a fluid flow channel design with a micropillar array inside

with a 20×20 mm, 0.35 mm deep recess. The mold was passivated and fixed against a silicon wafer with the clamp. The titanium mold was not prone to deformations or leaks, and yielded PDMS micropillar arrays of a consistent geometry over all experiments (Fig. 5.11d).

PDMS micropillar arrays for fluid flow channels

Subsequently we established the production of PDMS micropillar arrays that met earlier described requirements. Briefly, the titanium mold and the silicon wafer were passivated and brought into contact. The two parts were fixed with a clamp (Fig. 5.4a). PDMS, that was previously degassed, was pressed into one of the two openings of the mold using a pipette (Fig 5.4b). The whole assembly was degassed in a vacuum chamber to avoid air bubbles on top of the wafer. Subsequently the PDMS was cured for 20 hours at 110°C (Fig. 5.4c). The mold was detached from the wafer (Fig. 5.4d), and the PDMS micropillar array was pealed off the silicon wafer (Fig. 5.4e). Excess PDMS was cut off with a sharp blade to leave a 10×10 micropillar array flanked by two 10×2 mm, 50 μm high spacers (Fig. 5.4f). The micropillar array was subsequently divided into two halves along the long side (Fig. 5.4g). The middle

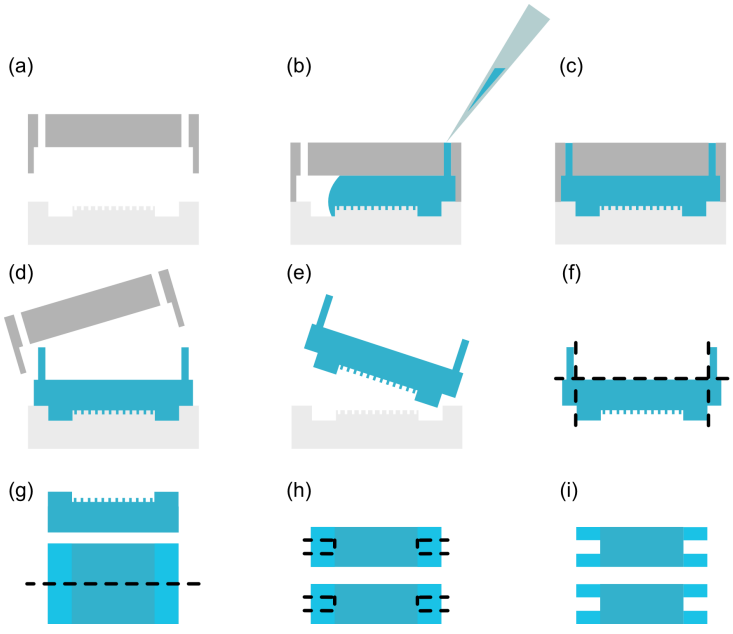

Figure 5.4: A schematic representation of how PDMS micropillar arrays have to be prepared to fit in fluid flow channels. (a) First step is to passivate and fix the mold and a silicon wafer against each other. (b) Second step is to degas PDMS and insert it into the mold. (c) Third step is to degas PDMS in the mold and cure for 20 hours under 110°C. (d, e) Fourth step is to detach the mold from the wafer and pill off the PDMS micropillar array. (f) Fifth step is to cut excess of PDMS and leave only micropillar array with flanking spacers. (g) Sixth step is to divide PDMS micropillar array in two halves. (h, i) Seventh step is to cut off the middle parts from spacers

parts of the spacers $\sim 1.7\ mm$ wide were cut out to allow fluid flow to pass through (Fig. 5.4h, i). In this way two micropillar arrays for two channels were prepared in one step.

Subsequently all parts were assembled and tested. Additional PDMS was added to the bottom of the micropillar arrays to "glue" them inside the channels. For assembly a small amount of PDMS with a 1:30 crosslinker-base ratio was spread inside each channel of the slide (Fig. 5.5a). The PDMS micropillar arrays were placed on top of the spread PDMS. Pressure was applied to the spacers to make sure arrays were properly deepened in the channels (Fig. 5.5b). The slide was further cured at 60°C for 30 minutes. Then, micropillar arrays were functional-

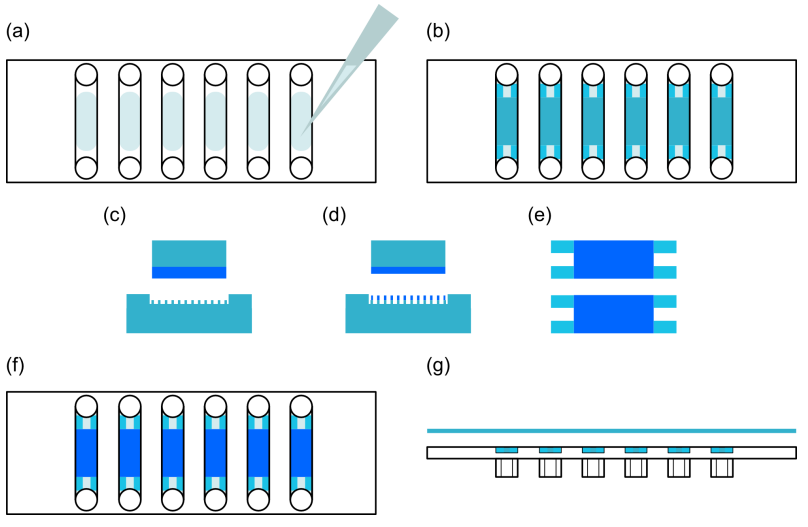

Figure 5.5: A schematic representation of fluid flow channels assembling with micropillar arrays. (a) First step is to spread a small amount of 1:30 PDMS in channels. (b) Second step is to put prepared PDMS micropillar array inside the channels and cure for 30 min at 60°C. (c-f) Third step is to functionalize micropillar arrays with a fluorescently labeled protein of interest. (g) Fourth step is to close channels with a coverslip, passivate micropillar arrays and wash channels with PBS.

ized with the help of PDMS stamps with fluorescently labeled fibronectin on top of them (Fig. 5.5c-f). Finally, channels were closed off with a coverslip (Fig. 5.5g). The whole assembly was passivated and washed with PBS. Tests using colored water showed that the assembly was tight, and that a continous fluid flow could be supported (Fig. 5.12).

Seeding cells on micropillar arrays inside fluid flow channels

Further the work flow for seeding cells on PDMS micropillar arrays inside the closed fluid flow channels was designed but not tested. Channels will be washed with PBS (Fig. 5.6a). Then, approximately 20000 cells will be flushed via the channel entrances into the chamber (Fig. 5.6b). Channels are closed with the lids provided. The distribution of cells on the PDMS micropillar arrays would be analysed using a microscope (Fig. 5.6c). If the cell density is satisfying, the slide with the channels can be flipped over to allow cells to sink to the top of the mi-

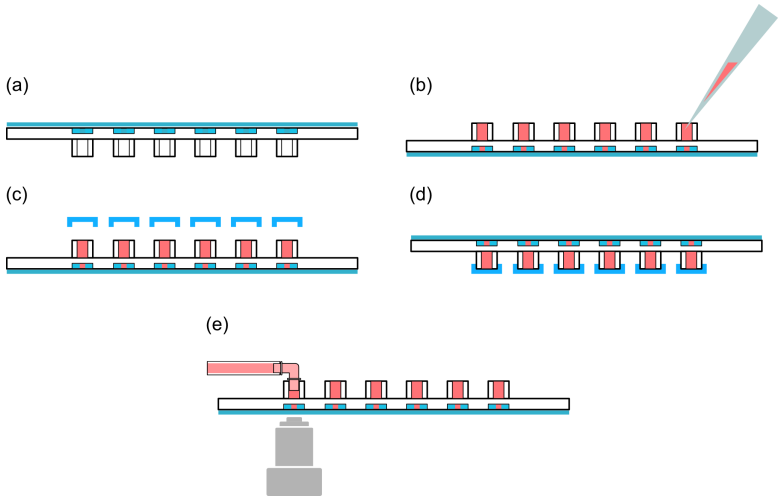

Figure 5.6: A schematic representation of seeding and imaging cells inside fluid flow channels. (a) An earlier prepared slide with PDMS micropillar arrays shall be washed with PBS. (b) A cell culture media containing 20000 cells per sample shall be inserted via channel openings. (c) Fluid flow channels have to be closed with provided lids and cell distribution shall be checked under the microscope (d) The slide has to be inverted to allow cells sink on top of the micropillar arrays. (e) After 1 hour incubation cells can be imaged with a connected fluid flow system

cropillar arrays (Fig. 5.6d). After 1 hour of incubation the slide can be flipped back and imaged under the microscope with a connected fluid flow system (Fig. 5.6e).

5.3.5 Fluid flow in a microchannel with pillars

Finally, we determined the properties of the fluid flow in the channel with micropillar arrays mounted. We required that fluid flow to be laminar, as described by it's Reynolds number. The Reynolds number for the channel was calculated for water at 37 °C in a range of fluid volumetric flow rates (Q) from 0 ml/min to 100 ml/min (Fig. 5.7). The Reynolds number is the ratio between the inertial forces in a fluid and the viscous forces, characterizing the boundary between laminar flow (here desired) and turbulent flow (to be avoided). The Reynolds number, Re is given by [19]:

$$Re = \frac{QD_H\rho}{\mu A}$$

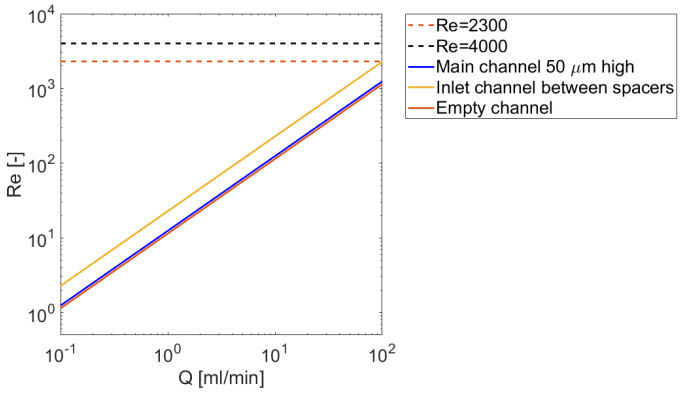

Figure 5.7: Reynolds number in different parts of the channel plotted for water at 37°C over volumetric flow rate.

where Q is the fluid volumetric flow rate, D_H the hydraulic diameter, ρ the density of the fluid, μ the dynamic viscosity, and A the cross sectional area of the channel. For noncircular pipes or channels the hydraulic diameter D_H is given by [19]:

$$D_H = \frac{4A}{P} = \frac{4ab}{2(a+b)} = \frac{2ab}{a+b}$$

where A is the cross sectional area of the channel, P the wetted perimeter, a the hight, and b the width of the channel.

Our calculations showed that fluid flow is laminar in all parts of the channel, given the envisioned flow rates and the design parameter: in the part without micropillar array, in between the spacers, and in the area with the pillars 0 μm high (Fig. 5.7). We performed this analysis for arrays of 3.8 μm (Fig. 5.8a) and 12 μm high pillars (Fig. 5.8b). As can be seen from the graphs, the Reynolds number stays low, hence the flow stays laminar using micropillars of different heights at volumetric flow rates of $0 - 100$ ml/min. At those flow rates the volume below the pillars can be exchanged as fast as 30 ms for the highest flow-rates.

Further, we determined the hydrodynamic entry length of liquid at 37°C inside the channel, i.e. between 0 μm, 3.8 μm and 12 μm high (Fig. 5.9). The entry length describes the distance from the entrance of the channel where the wall shear stress and friction factor reach about 2% of the fully developed value. It therefore describes the spreading of the laminar flow over the full channel diameter after entering a volume. It

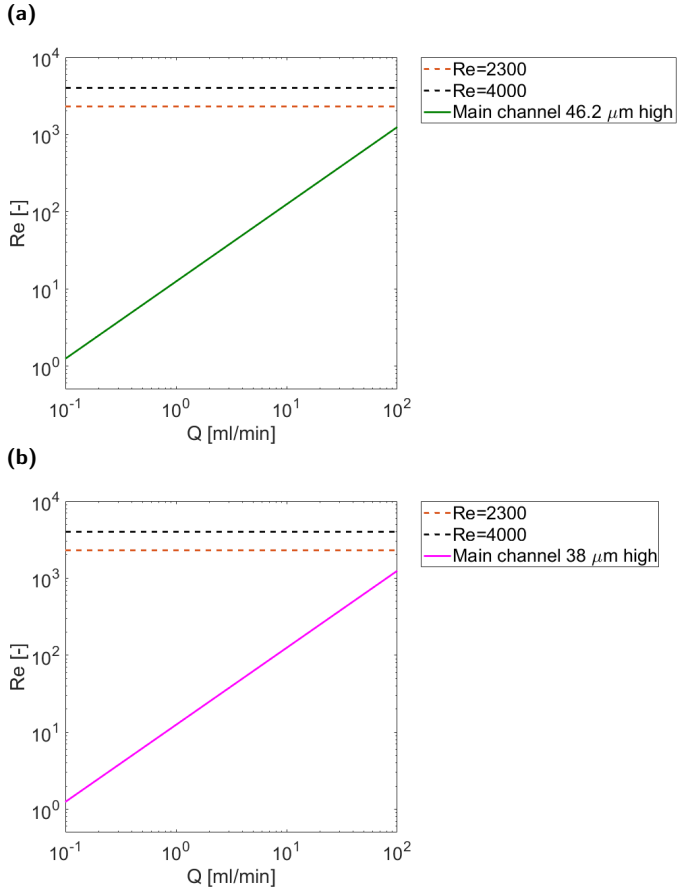

Figure 5.8: Reynolds number for a channel with micropillars (a) 3.8 μm high and (b) 12 μm high plotted over volumetric flow rate

is important for our experiments that the hydrodynamic entry length is small in comparison to the length of the micropillar arrays, being 10 mm. For a laminar flow the hydrodynamic entry length is given by [19]:

$$L_{h,laminar} \cong 0.05\ Re\ D_H$$

The calculations for our channel design shows that entry length will reach half of the channel with micropillars at about 80 ml/min volumetric flow rate and higher (Fig. 5.9).

Finally, we estimated the volumetric flow rate of liquid at 37°C at which the shear stress exerted on the channel wall with pillars will be

in a physiological for cells range – between 0 and 1 Pa [20, 21]. For Newtonian fluids shear stress is expressed as

$$\tau = \mu \frac{dU}{dh}$$

where μ – dynamic viscosity, $\frac{dU}{dh}$ – velocity gradient [19]. Taking into the account that fluid velocity between two plates is

$$\frac{U}{U_{max}} = 1 - (\frac{2h}{H})^2$$

where U_{max} – maximum velocity, which occurs at the centreline, H – channel hight, h – distance from the centreline [19]. Dependency of the shear stress and the volumetric flow rate can be expressed as

$$Q = \frac{AU_{max}}{2} = \frac{ab\tau H^2}{\mu 16h}$$

Our results suggest that shear stress will reach 1 Pa in a channel without pillars at a volumetric flow rate of $\sim 100\ \mu m/min$ (Fig. 5.10). At this flow rate the Reynolds number and the hydrodynamic entry length are negligible for water at 37 °C inside the 50 μm high channel – 1.243 and $6,134\ \mu m$ respectively. Thus, cellular forces can be reliably measured over $\sim 99,87$ % of the micropillar array area.

5.4 Discussion

Currently, the mechanical properties of pericytes (PCs), although of significant importance to their biological function, can only be inferred from (post mortem) *in vivo* imaging. The main reason for this lack of acessibility is the difficulty of generating homogeneous cell culture of primary mid-capillary PCs, as they show differences in phenotype and expression of proteins depending on their location on the capillary tree and don't have unique markers [22–24]. Additionally, "true" or "approved" PCs are located on mid-capillaries that show the most clear differences from smooth muscle cells (SMCs) [1, 22]. PCs located on pre- or post-capillaries have been defined as "transitional" PCs [24]. Thus, generating a cell culture of "true", mid-capillary, primary PCs that don't show expression of α-SMA and support angiogenesis is nearly impossible. As

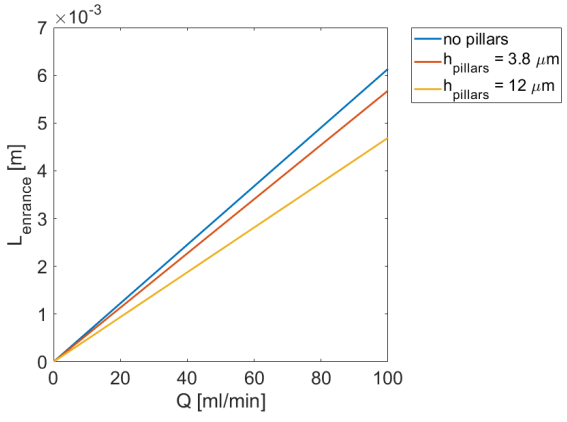

Figure 5.9: Hydrodynamic entry length of water at 37°C inside the channel part with micropillars 0 μm, 3.8 μm and 12 μm high

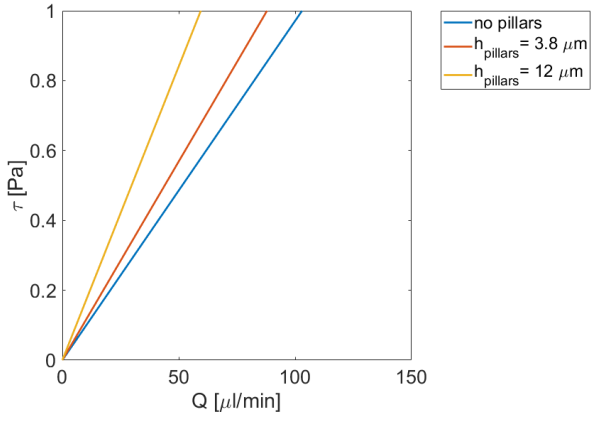

Figure 5.10: Shear stress of water on the wall at 37°C inside the channel part with micropillars 0 μm, 3.8 μm and 12 μm high

a confirmation, there are no such commercially available primary PCs present.

In vivo experiments lack the level of control of experimental conditions and don't support direct cell force measurements in contrast to *in vitro* studies. In the case of PCs it is particularly unfortunate, as their contractility was spotted to be involved, among others, in regulation of capillary diameter, cerebral blood flow or promote brain damage in ischemia [3–5].

Here, we made an attempt to close this gap by using hiPSC-derived PCs that resemble "true" PCs located on mid-capillaries, characterized by lack α-SMA and that support angiogenesis [10, 11]. In combination with PDMS micropillar array technology we performed *in vitro* cell force measurements of PCs in reproducible hypoxia and ischemia conditions. Hypoxic oxygen deprivation was initially simulated with the help of DMOG. By additional subtraction of glucose from the cell culture media we reproduced ischemia conditions.

Our results showed that PCs in starvation condition, retained their morphology and spreading behavior in comparison to the control condition, yet displayed a somewhat lower force application. Thus starvation had only a minor effect on the cell's mechanical properties. Hypoxia was paralleled by an increase of cell spreading and simultaneous significant decrease in cellular force generation. In ischemia cell spreading area decreased significantly, while cellar force application partially recovered.

Those results only in part follow the predicted behavior. As described in literature [3], PCs will constrict and die in ischemic conditions after one hour. Hence, we hypothesized that PCs had a higher force application and a smaller cell spreading area in ischemic condition. While the first expectation was confirmed by our data, the latter does not. We do suspect that this result is due to the way we simulated ischemia which first needed a long incubation step with DMOG leading to hypoxia, followed by the final low-glucose situation. The increase of force exertion compared with hypoxia might be in agreement with this hypothesis.

Our results showed that this method doesn't allow to register fast changes in the behaviour of PCs and mimic ischemia as an immediate event in time. To perform live cell force measurements the in house designed micropillar arrays had to be flipped over [12]. However, our investigation revealed that liquid exchange under the array is not sufficiently fast. Due to the small opening between the coverslip and mi-

cropillars (50 μm) that is required for high resolution measurements of cellular forces the liquid exchange depends only on diffusion.

Therefore, we designed and characterized a new approach that allows us to constantly monitor cellular forces during rapidly exchange of cell culture media to expose cells to different conditions. Our approach combines commercially available fluid flow channels with the in house designed micropillar arrays. The fluid flow properties inside this channel with integrated micropillar array, showed that cellular forces can be reliably measured over $\sim 99,87$ % of the micropillar array area at a physiological for cells shear stress during the liquid exchange.

Taken together, our approach can complement *in vivo* studies on PC behaviour in hypoxia and ischemia conditions and be used for other applications where cell mechanobiology under changing fluid flow or cell media composition is of interest.

5.5 Apendix

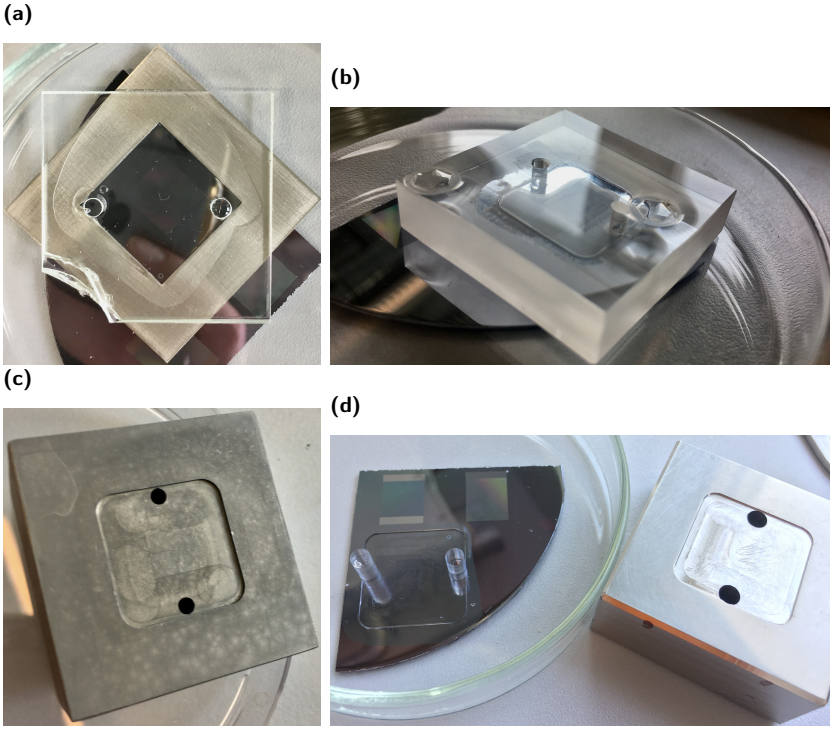

Figure 5.11: Additional molds for PDMS micropillar arrays after testing.(a) Mold made of a combination of glass slide and stainless still frame was prone to PDMS leaks. (b) Mold made of a poly(methyl methacrylate) (PMMA) got deformations after curing at 110°C in places were clamp was attached. (c) Stainless still frame got signs of corrosion after passivation with trichlorosilane. (d) Titanium mold showed overall good results

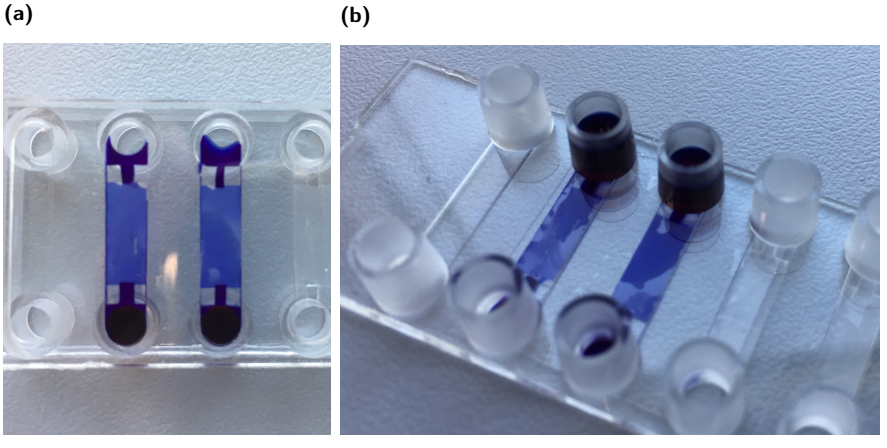

Figure 5.12: Test of the fluid flow channels with PDMS micropillar arrays inside. (a) μQ water coloured with a dye inside fluid flow channels with PDMS micropillar arrays - slide bottom view. (b) Slide top view shows water passing not only between micropillars and a coverslip, but also under the bottom of the micropillar arrays

Bibliography

[1] Annika Armulik, Guillem Genové and Christer Betsholtz. « Pericytes: developmental, physiological, and pathological perspectives, problems, and promises. » In: *Dev. Cell* 21.2 (2011), pp. 193–215. ISSN: 1534-5807.

[2] Bryan L. Krock, Nicolas Skuli and M. Celeste Simon. « Hypoxia-Induced Angiogenesis Good and Evil ». In: *Genes & Cancer* 2.12 (2011), pp. 1117–1133. ISSN: 1947-6019.

[3] Catherine N Hall et al. « Capillary pericytes regulate cerebral blood flow in health and disease. » In: *Nature* 508.7494 (2014), pp. 55–60. ISSN: 0028-0836.

[4] Anusha Mishra et al. « Astrocytes mediate neurovascular signaling to capillary pericytes but not to arterioles. » In: *Nat. Neurosci.* 19.12 (2016), pp. 1619–1627. ISSN: 1097-6256.

[5] Robert A Hill et al. « Regional Blood Flow in the Normal and Ischemic Brain Is Controlled by Arteriolar Smooth Muscle Cell Contractility and Not by Capillary Pericytes. » In: *Neuron* 87.1 (2015), pp. 95–110. ISSN: 0896-6273.

[6] Gregg L. Semenza. « Life with Oxygen ». In: *Science* 318.5847 (2007), pp. 62–64. ISSN: 0036-8075.

[7] Agnieszka Loboda, Alicja Jozkowicz and Jozef Dulak. « HIF-1 versus HIF-2 – Is one more important than the other? » In: *Vascular Pharmacology* 56.5-6 (2012), pp. 245–251. ISSN: 1537-1891.

[8] Frédéric Dayan et al. « Gene regulation in response to graded hypoxia: the non-redundant roles of the oxygen sensors PHD and FIH in the HIF pathway. » In: *Journal of theoretical biology* 259.2 (2009), pp. 304–16. ISSN: 0022-5193.

[9] Theodore Kalogeris et al. « Chapter Six Cell Biology of Ischemia / Reperfusion Injury ». In: *International Review of Cell and Molecular Biology* 298 (2012), pp. 229–317. ISSN: 1937-6448.

[10] Akhilesh Kumar et al. « Specification and Diversification of Pericytes and Smooth Muscle Cells from Mesenchymoangioblasts ». In: *Cell Reports* 19.9 (2017), pp. 1902–1916. ISSN: 2211-1247.

[11] Valeria V Orlova et al. « Functionality of Endothelial Cells and Pericytes From Human Pluripotent Stem Cells Demonstrated in Cultured Vascular Plexus and Zebrafish Xenografts ». In: *Arteriosclerosis Thrombosis Vasc Biology* 34.1 (2014), pp. 177–186. ISSN: 1079-5642.

[12] Hedde van Hoorn et al. « The Nanoscale Architecture of Force-Bearing Focal Adhesions ». In: *Nano letters* 14 (2014), pp. 4257–4262.

[13] Olivia du Roure et al. « Force mapping in epithelial cell migration. » In: *Proc. Natl. Acad. Sci. U.S.A.* 102.7 (2005), pp. 2390–5. ISSN: 0027-8424.

[14] John L Tan et al. « Cells lying on a bed of microneedles: an approach to isolate mechanical force. » In: *Proc. Natl. Acad. Sci. U.S.A.* 100.4 (2003), pp. 1484–9. ISSN: 0027-8424.

[15] Jianping Fu et al. « Mechanical regulation of cell function with geometrically modulated elastomeric substrates. » In: *Nat. Methods* 7.9 (2010), pp. 733–6. ISSN: 1548-7091.

[16] YA Minamishima, J Moslehi and RF Padera. « A feedback loop involving the Phd3 prolyl hydroxylase tunes the mammalian hypoxic response in vivo ». In: (2009).

[17] Alexander Weidemann et al. « HIF-1α activation results in actin cytoskeleton reorganization and modulation of Rac-1 signaling in endothelial cells ». In: *Cell Communication and Signaling* 11.1 (2013), p. 80.

[18] Xian-Bao Liu et al. « Prolyl hydroxylase inhibitor dimethyloxalylglycine enhances mesenchymal stem cell survival ». In: *Journal of Cellular Biochemistry* 106.5 (2009), pp. 903–911. ISSN: 1097-4644.

[19] Yunus A. Çengel and John M. Cimbala. *Fluid Mechanics: Fundamentals and Applications*. English. 4th ed. New York: McGraw-Hill Education, 2017. ISBN: 9781259696534.

[20] James N. Topper and Michael A. Gimbrone Jr. « Blood flow and vascular gene expression: fluid shear stress as a modulator of endothelial phenotype ». In: *Molecular Medicine Today* 5.1 (1999), pp. 40–46. ISSN: 1357-4310.

[21] Cara F Buchanan et al. « Flow shear stress regulates endothelial barrier function and expression of angiogenic factors in a 3D microfluidic tumor vascular model ». In: *Cell Adhesion & Migration* 8.5 (2015), pp. 517–524. ISSN: 1933-6918.

[22] V Nehls and D Drenckhahn. « Heterogeneity of microvascular pericytes for smooth muscle type alpha-actin. » In: *JCB* 113.1 (1991), pp. 147–154. ISSN: 0021-9525.

[23] Roger Grant et al. « Organizational hierarchy and structural diversity of microvascular pericytes in adult mouse cortex ». In: *J Cereb Blood Flow Metabolism* 39.3 (2017), pp. 411–425. ISSN: 0271-678X.

[24] K.W. Zimmermann. « Der feinere bau der blutcapillares ». In: *Z. Anat. Entwickl.* 68 (1923), pp. 3–109.